Raman study of tetragonal $TbPO_4$ and observation of a first-order phase transition at high pressure

2008 J. Phys.: Condens. Matter 20 425216

(http://iopscience.iop.org/0953-8984/20/42/425216)

J. Phys.: Condens. Matter **20** (2008) 425216 (7pp) doi:10.1088/0953-8984/20/42/425216

Raman study of tetragonal $TbPO_4$ and observation of a first-order phase transition at high pressure

A Tatsi, E Stavrou, Y C Boulmetis, A G Kontos, Y S Raptis and C Raptis[1]

Department of Physics, National Technical University of Athens, GR-15780 Athens, Greece

E-mail: craptis@central.ntua.gr

Received 9 July 2008, in final form 7 August 2008
Published 25 September 2008
Online at stacks.iop.org/JPhysCM/20/425216

Abstract

The Raman spectra of tetragonal $TbPO_4$ (zircon-type $I4_1/amd$ structure, D_{4h}^{19} space group) have been measured at ambient conditions and under variable pressure up to 15.5 GPa inside a diamond anvil cell (DAC). Assignment of the Raman active modes of the tetragonal phase has been carried out based on polarized measurements from a single oriented crystal of $TbPO_4$ at ambient conditions. The abrupt Raman mode discontinuities and the appearance of numerous new Raman peaks at a pressure $P_c \approx 9.5$ GPa have provided strong evidence for a first-order phase transition to a lower crystal symmetry, most likely monoclinic. The high-pressure structure appears to be more compact compared to the tetragonal one, and is retained upon bringing the crystal to ambient pressure.

(Some figures in this article are in colour only in the electronic version)

1. Introduction

Terbium phosphate ($TbPO_4$), along with several other RPO_4 (R = heavy rare-earth ion, Tb to Lu) compounds, normally crystallizes in the tetragonal zircon ($ZrSiO_4$) $I4_1/amd$ (D_{4h}^{19}) structure [1–3] at ambient conditions, with two formula units in the primitive cell. In this structure, the phosphorus atoms are four-fold coordinated by oxygen forming tightly bound $(PO_4)^{3-}$ tetrahedral units, while the Tb^{3+} cations have an eight-fold coordination to oxygen in the shape of TbO_8 dodecahedra. The two types of polyhedra are lined up in an edge-sharing linkage producing linear chains along the c axis [3]. Both the Tb^{3+} and $(PO_4)^{3-}$ ions are located in D_{2d} symmetry sites, while the oxygen atoms occupy C_s symmetry sites. In contrast, the light rare-earth ion RPO_4 compounds (R = La to Gd), are known [2, 3] to crystallize in the monoclinic monazite ($CePO_4$) $P2_1/n$ (C_{2h}^5) structure, with four molecules in the primitive cell. This is a distorted, but more compact, zircon structure as the coordination number of the rare-earth ion increases to 9, with the formation of RO_9 polyhedra [3] in place of RO_8 dodecahedra.

A dimorphism is known to exist [4, 5] at ambient conditions for some RPO_4 compounds (including $TbPO_4$) which, depending on the preparation conditions, can be grown in either the zircon or monazite structure. This is not unexpected, bearing in mind that the two structures are, crystallographically, closely related. In addition, measurements of the enthalpies of formation for RPO_4 crystals by Ushakov *et al* [5] imply that the zircon-structured $TbPO_4$ is thermodynamically more stable than the monazite-type dimorph, with the energy difference between the two structures being very low. In fact, monazite-type $TbPO_4$ is known [4] to transform to a zircon-type structure at elevated temperatures.

$TbPO_4$ has attracted considerable interest in the past for its remarkable magnetic properties [6–11] and phase transitions [6–8, 10] at low temperatures. In particular, at $T_N = 2.28$ K, this crystal displays an antiferromagnetic ordering [6, 7] parallel to the c-axis of the tetragonal phase, followed closely, at $T = 2.15$ K, by another change [6, 7] of its magnetic structure in which the spin moments tilt collinearly off the c-axis in the (110) plane. The magnetic moment tilting is accompanied by a structural distortion in which the crystal symmetry is lowered from tetragonal to, most likely, monoclinic [7]. The structural phase transition has been

[1] Author to whom any correspondence should be addressed.

attributed [7, 10] to anharmonic coupling of lattice modes with electronic states of the Tb^{3+} cations at low temperatures, in which a splitting of the ground electronic level of the Tb^{3+} cations is caused by the crystal field (*cooperative Jahn–Teller effect* [12, 13]).

The high-pressure phase transitions of ABO_4 compounds have been studied extensively in the past for a variety of crystal structures and the results of such studies were reviewed in a relevant monograph [14] about two decades ago. A general conclusion of those studies [14] is that the radii ratios r_A/r_O and r_B/r_O between cations and oxygen increase with pressure, resulting in an increase of cation coordination in the high-pressure modifications.

Most of the zircon-type ABO_4 compounds are known [14–20] to undergo a phase transition at high pressure to a tetragonal scheelite ($CaWO_4$) $I4_1/a$ (C^6_{4h}) structure. Indeed, x-ray [15–17] and Raman [16, 18–20] studies of the zircon crystal ($ZrSiO_4$) itself [15], rare-earth vanadates [16–18] as well as some isomorphous $XCrO_4$ (X = Ca, Y) chromates [19, 20] have indicated an irreversible transition to the more compact scheelite structure. However, on some occasions [14, 21–23], namely for zircon-structured $CeVO_4$ and $ThSiO_4$, the first pressure-induced transition is definitely to the monazite structure, which, in the case of $CeVO_4$, is followed by a second transition [21, 22] to the scheelite structure at a higher pressure. In fact, the sequence zircon → monazite → scheelite was suggested [14] as a likely pressure-driven route for zircon-structured $A^{3+}B^{5+}O_4$ crystals. Furthermore, in $A^{2+}B^{6+}O_4$ compounds displaying ambient conditions structures other than the zircon-type one, an intermediate phase sequence zircon → monazite → scheelite was also reported [14]. Actually, such pressure-induced transitions are compatible with an increasing structural compactness along this sequence [14, 21].

There have been no reports so far about any structural changes of rare-earth phosphates at high pressures. In a recent review article [4] dealing with the stability ranges of RXO_4 (X = P, As, V) compounds, RPO_4 crystals are considered stable at high pressures. More recently [24], the Raman spectrum of zircon-structured $DyPO_4$ was measured up to 7.5 GPa, without any definite evidence for a phase transition up to this pressure; apart from this report [24], there are no previous high-pressure studies on any other rare-earth phosphate.

Group theory predicts 12 Raman active modes for the zircon structure of $TbPO_4$ with A_{1g}, B_{1g}, B_{2g} and (doubly degenerate) E_g symmetries corresponding to the following Raman (polarizability) tensor components [1]:

$$A_{1g} = \begin{pmatrix} xx & & \\ & yy & \\ & & zz \end{pmatrix} \qquad B_{1g} = \begin{pmatrix} xx & & \\ & -yy & \\ & & \end{pmatrix}$$

$$B_{2g} = \begin{pmatrix} & xy & \\ yx & & \\ & & \end{pmatrix} \qquad E_g = \begin{pmatrix} & & xz \\ & & yz \\ zx & zy & \end{pmatrix}.$$

Seven of these modes ($2A_{1g} + 2B_{1g} + B_{2g} + 2E_g$) are classified [1, 2] as *internal* due to normal vibrations of oxygen atoms within the $(PO_4)^{3-}$ tetrahedral units, four ($2B_{1g} + 2E_g$) as *external translational* (pure lattice modes) arising from translations of $(PO_4)^{3-}$ and Tb^{3+} ions and one (E_g) as *rotational* of whole $(PO_4)^{3-}$ units. Based on symmetry considerations, Dawson *et al* [1] produced the atomic displacements of all the normal modes of the zircon structure.

The ambient conditions Raman spectra of zircon-structured orthophosphates (including $TbPO_4$) were reported by Begum *et al* [2], who also made mode assignments by performing polarized Raman measurements on single, oriented crystals. However, from similar polarized measurements on some of these compounds, Elliott *et al* [12] (for $DyPO_4$) and Becker *et al* [25] (for $ErPO_4$ and $TmPO_4$) concluded (partially) different symmetry assignments (from those of Begum *et al* [2]) for a few Raman modes.

In this paper, we present Raman scattering data from single crystals of $TbPO_4$ at (1) ambient conditions, and (2) under variable pressure up to 15.5 GPa in both increasing/decreasing pressure cycles. At ambient conditions, polarized spectra have been obtained from an oriented single crystal which enabled us to assign the Raman modes of $TbPO_4$. Abrupt spectral changes observed at a pressure $P_c \approx 9.5$ GPa imply a first-order phase transition to a lower symmetry structure, which is quenchable upon pressure release.

2. Experimental details

A rectangular ($3 \times 4 \times 4$ mm^3) flux grown, oriented single crystal of tetragonal $TbPO_4$ cut along the crystallographic axes was used for the ambient conditions polarized Raman measurements which were performed at a 90° scattering geometry, allowing the recording of the following four spectral components: $y(zz)x$, $z(xx)y$, $z(yx)y$ and $z(yz)y$, giving all the expected mode symmetries of the crystal: A_{1g}, ($A_{1g} + B_{1g}$), B_{2g} and E_g, respectively. In the above notation, the laboratory frame axes x, y, z coincide on every occasion with the crystallographic axes a, b, c. For simplicity, the above components will be referred to, from now on, by the (polarization) symbols inside the parenthesis. Small pieces of $TbPO_4$, cut from the bulk single crystal, with nominal dimensions 50–80 μm, were loaded into a diamond anvil cell (DAC) along with ruby chips for monitoring the pressure. A Syassen–Holzapfel-type DAC [26] was used equipped with two sapphire optical windows on either side of the diamond set up, one at the entrance served to direct (after refraction) the exciting laser beam to nearly normal incidence to the entrance diamond and the other at the back to allow visual observation of the sample area. The metal gasket between the two diamonds had a hole of ~200 μm in diameter which was filled with a 4:1 methanol–ethanol pressure transmitting medium. The latter provides good hydrostatic conditions up to a pressure of 10 GPa (at which it solidifies) and quasi-hydrostatic ones above this pressure, and these facts have been confirmed by the absence of significant broadening of the ruby PL bands. Raman data were obtained up to 15.5 GPa in several experimental sessions of increasing and decreasing pressure cycles.

The Raman spectra were excited by the 514.5 nm line of an Ar^+ laser at a power of ∼400 mW measured at the entrance of the DAC, with the actual power level at the sample being lower because of losses in the sapphire window of the DAC. Since both $TbPO_4$ and pressure transmitting medium are transparent materials, sample heating was negligible and this was confirmed by the absence of any Raman mode shifting in $TbPO_4$ when the latter was excited inside the DAC at ambient conditions. The above excitation line was considered optimum since the level of photoluminescence (PL) emission excited with this line was low and affected only the high-frequency part of the spectrum ($\omega > 1000$ cm^{-1}). The broad PL emission, which had also been observed previously [2], decreased with increasing pressure, but reappeared weakly after pressure release. To verify the nature of this emission and clearly observe the Raman peaks, we also used, in measurements outside the DAC, the 647.1 nm line of a Kr^+ laser.

A nearly back-scattering Raman geometry was used for the high-pressure experiments in which scattered light from the DAC was analysed and detected by a SPEX double monochromator in conjunction with a cooled photomultiplier and photon counting equipment. Most of the high-pressure Raman measurements were not polarized, thus allowing all phonon symmetry species to appear in each spectrum scan. However, in order to resolve two phonon peaks whose frequency–pressure plots cross, detailed slow-scan measurements were conducted in parallel- and cross-polarization configurations, over the corresponding spectral region and for pressures around the crossing. The spectral resolution of the system was about 3 cm^{-1} in all experimental sessions.

3. Results and discussion

3.1. Ambient conditions spectra and mode assignments

Figure 1 shows unpolarized Raman spectra of $TbPO_4$ at ambient conditions excited by the 514.5 nm Ar^+ (a), or the 647.1 nm Kr^+ (b) laser line, respectively; in either spectrum of figure 1, eleven (out of twelve) Raman modes of $TbPO_4$ appear and their symmetry assignments (based on polarized Raman measurements presented below) are given. In the high-frequency region (970–1300 cm^{-1}), broad spectral features are readily noticed when the green Ar^+ laser line is used (figure 1(a)) obscuring clear observation of, at least, two modes. These features disappear when excitation is realized by the red Kr^+ laser line (figure 1(b)), thus indicating that they are PL bands; the likely origin of these PL bands is discussed below in section 3.2. When the Kr^+ laser is used for excitation, the three high-frequency internal modes of $TbPO_4$ are clearly recorded at 995, 1014 and 1049 cm^{-1} (figure 1(b)) and can be identified in the corresponding spectrum excited by the green Ar^+ laser line (figure 1(a)). Unfortunately, the red Kr^+ laser line is not suitable for the present high-pressure setup because of a strong overlap of the high-frequency Raman spectrum of $TbPO_4$ with the ruby PL calibration bands. However, as discussed below, the intensity of the PL bands of $TbPO_4$ gradually decreases with increasing pressure. The weak band

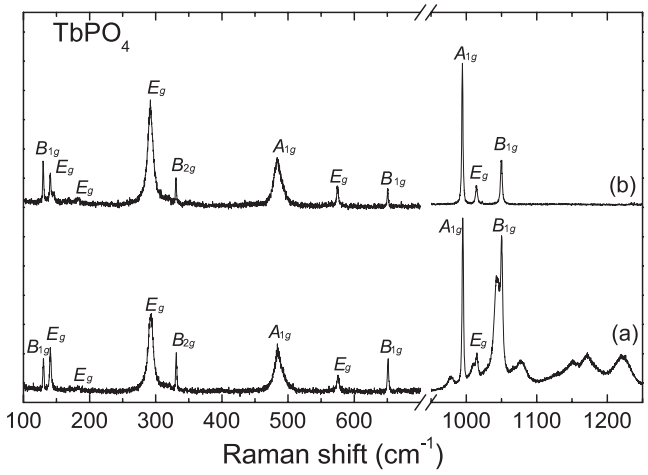

Figure 1. Unpolarized Raman spectra of $TbPO_4$ excited by the 514.5 nm Ar^+ (a) and 647.1 Kr^+ (b) laser lines showing eleven Raman modes of the crystal. The high-frequency broad peaks in (a) are luminescence bands which disappear when the red Kr^+ laser line (b) is used for excitation.

at 185 cm^{-1}, which is on the verge of detection in both spectra of figure 1, has also been weakly recorded in polarized Raman measurements presented below.

The zz, xx, yx and yz polarized components of the Raman spectrum of $TbPO_4$ at ambient conditions are shown in figure 2, giving primarily A_{1g}, (A_{1g} + B_{1g}), B_{2g} and E_g symmetry modes, respectively. In the zz component, two Raman peaks are clearly evident at 484 and 995 cm^{-1} and assigned as A_{1g} symmetry modes, while in the yx component there is only one definite Raman peak at 331 cm^{-1} corresponding to the sole B_{2g} mode of the crystal. The above components contain negligible polarization leakages from different symmetry modes. In the xx component (figure 2), both A_{1g}- and B_{1g}-type modes are expected and, excluding the strong peaks at 484 and 995 cm^{-1} (already assigned as A_{1g} modes), there are three additional strong Raman peaks at 141, 649 and 1049 cm^{-1} which appear exclusively in this component; because of this, the latter bands are assigned as B_{1g} symmetry modes. Further, in the xx component, weaker bands at 130, 293 and 576 cm^{-1} are also evident which are considered polarization leakages of E_g symmetry modes; indeed, these bands appear stronger in the yz component and, hence, should correspond to E_g modes. In addition, in the yz spectrum (figure 2), the strong narrow band at 1014 cm^{-1} (observed only in this configuration) is also assigned as an E_g mode.

The weak band at 185 cm^{-1} is observed in both xx and yz components with comparable intensity levels, as depicted from the detailed spectral profiles given in the inset of figure 2. In fact, the intensity of this band appears higher (by about 25%) in the yz component, thus implying a, more likely, E_g symmetry mode; however, considering the large error margins corresponding to such a weak spectral peak, we do not exclude the possibility of it being a B_{1g} symmetry mode. It has not been possible to detect, in our spectra, the twelfth Raman mode of $TbPO_4$. Begum *et al* [2] reported a weak band at 267 cm^{-1} and assigned it as the fifth E_g mode of $TbPO_4$.

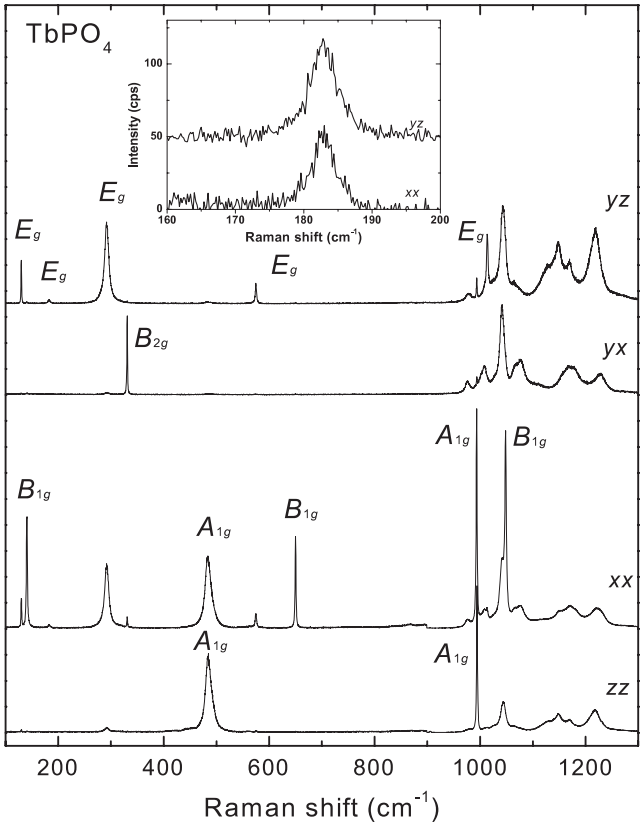

Figure 2. Polarized $y(zz)x$, $z(xx)y$, $z(yx)y$ and $z(yz)y$ Raman spectra of $TbPO_4$ at ambient conditions excited by the 514.5 nm Ar^+ laser line, giving primarily modes of A_{1g}, $(A_{1g} + B_{1g})$, B_{2g} and E_g symmetries, respectively. The intensity scales of all four spectra are the same up to 900 cm^{-1}, but above this frequency, the zz and xx spectra have been suppressed by a factor of 5, for clarity. The inset shows detailed parts of the xx and yz spectra, around the 185 cm^{-1} band, recorded at identical experimental conditions; the yz spectrum in the inset has been vertically displaced, for clarity.

Table 1. Ambient conditions frequencies ω_0, assignments, $(\partial\omega/\partial P)_T$ slopes and normalized $k = (1/\omega_0)(\partial\omega/\partial P)_T$ slopes of the Raman active modes of tetragonal $TbPO_4$.

ω_0 (cm^{-1})	Assignment	Character	$(\partial\omega/\partial P)_T$ (cm^{-1} GPa^{-1})	k (GPa^{-1})
130	E_g	Extern. transl.	−0.07	−0.54
141	B_{1g}	Extern. transl.	1.025	7.27
185	$E_g(B_{1g})$	Extern. transl.	0.10	0.54
293	E_g	Rotational	3.92	13.38
331	B_{2g}	Internal	−0.56	−1.69
484	A_{1g}	Internal	0.72	1.49
576	E_g	Internal	1.10	1.75
649	B_{1g}	Internal	1.98	3.05
995	A_{1g}	Internal	5.30	5.33
1014	E_g	Internal	5.00	4.93
1049	B_{1g}	Internal	5.30	5.05

The ambient conditions frequency values ω_0 of the eleven observed Raman modes, and their symmetry and character (internal, external) assignments are given in table 1, along with other useful quantities discussed below. Our mode assignments are almost in full agreement with those of Elliott *et al* [12] for $DyPO_4$, with the only uncertainty being the symmetry of the mode at 185 cm^{-1}. Further, our assignments differ partially from those of Begum *et al* [2] in the cases of two (or three) lowest-frequency modes, and Becker *et al* [25] for $ErPO_4$ and $TmPO_4$ in the cases of two high-frequency internal modes. The small differences appearing in the literature concerning the assignments of Raman modes of such compounds can be understood in terms of inter-component polarization leakages due to a slight misplacement or/and improper orientation of the single crystal. Also, in table 1, the character assignments (internal–external) are given for the observed modes which have been proposed in previous works [2, 12]; these assignments are justified by the mode groupings observed in the $(1/\omega_0)$ $(\partial\omega/\partial P)_T - \log\omega$ plots of the present work (see the following section).

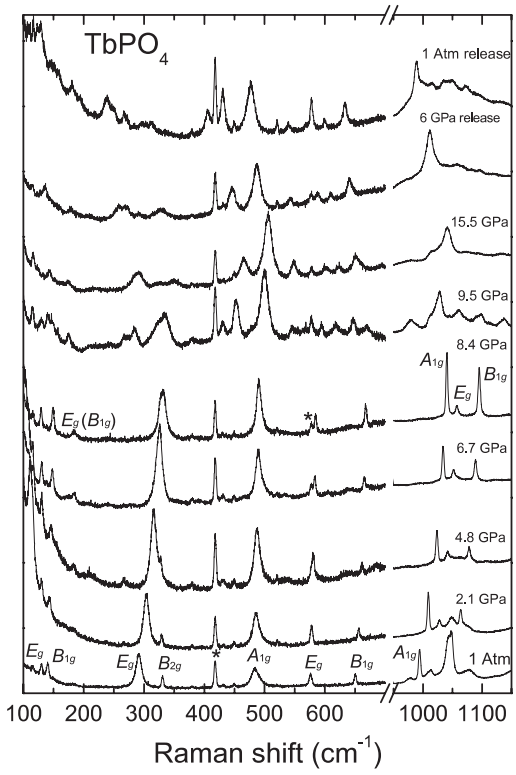

Figure 3. Raman spectra of $TbPO_4$ at various pressures in sequences of increasing–decreasing pressure cycles. *Raman peaks from sapphire window.

3.2. High-pressure spectra and phase transition

Unpolarized Raman spectra of $TbPO_4$ at several pressures (and also after pressure release) are presented in figure 3. Again, eleven Raman modes have been observed using the high-pressure setup. The pressure-independent peak observed at 418 cm^{-1} (figure 3) is due to Raman scattering from the sapphire (Al_2O_3) [27] window of the DAC and has been useful for spectral calibration. As the pressure is increased and the E_g Raman mode of $TbPO_4$ at 576 cm^{-1} hardens, a new peak emerges at 576.5 cm^{-1} which has been found (in separate scans with the DAC unloaded) to correspond also to a Raman mode of the sapphire [27] window, whose frequency happens

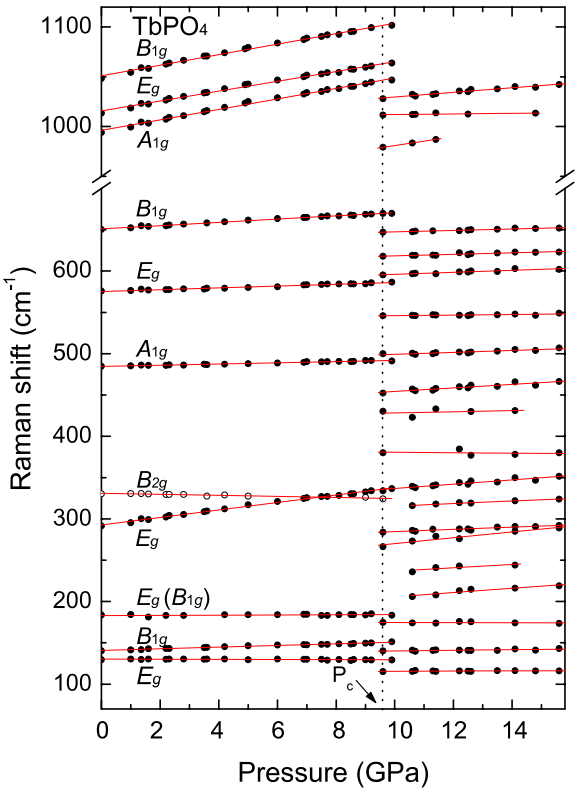

Figure 4. Frequency–pressure plots of the Raman active modes of $TbPO_4$ for the increasing pressure cycle. The solid lines correspond to linear least-squares fittings giving the $(\partial\omega/\partial P)_T$ slopes.

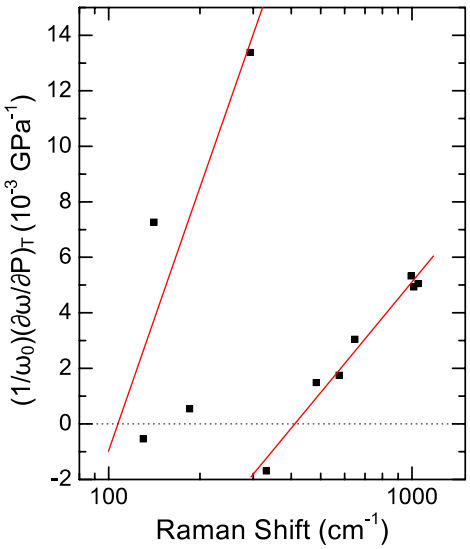

Figure 5. Linear–log plot of normalized $(1/\omega_0)$ $(\partial\omega/\partial P)_T$ slopes against mode frequencies for $TbPO_4$ showing the two separated groups (fittings) of internal (right) and external (left) modes.

to coincide with that of the E_g mode of $TbPO_4$ at ambient conditions. The mode at 185 cm^{-1} is barely detected at ambient pressure inside the DAC, but it picks up in intensity as the pressure is increased (figure 3). The PL bands in the high-frequency spectrum disappear above 4.5 GPa, emerge weaker at ∼9.5 GPa, then diminish gradually up to the highest pressure, and finally re-emerge weakly after pressure release (figure 3). These bands have also been observed in $TbPO_4$ by Begum *et al* [2], but without any comment about their origin; it is interesting that, among all the rare-earth phosphates (zircon- and monazite-type), $TbPO_4$ is the only member displaying PL bands at these energies. The pressure variation of the PL bands (disappearance and reappearance) indicates that they are, most likely, due to Tb^{3+} cation electronic transitions whose energy levels are sensitively tuned by pressure. Moreover, the fact the PL bands reappear at the phase transition implies that the energy levels are affected (reconstructed) by the new site symmetry of the Tb^{3+} cation and, generally, it appears they are sensitive to the crystal field of the structure in hand.

Plots giving the pressure dependence of all observed mode frequencies of $TbPO_4$ are shown in figure 4 over the entire increasing pressure cycle. The overlap of experimental points at the transition pressure P_c is, most likely, due to errors in the pressure determination over the various experimental runs. Linear fittings have been performed for the experimental points of each mode, from which $(\partial\omega/\partial P)_T$ and normalized $(1/\omega_0)$ $(\partial\omega/\partial P)_T$ slopes have been obtained for the low-pressure tetragonal phase and are listed in table 1. Since there are no elastic constants data available in the literature for $TbPO_4$, we have not been in a position to determine Grüneisen parameters γ_T for the phonons; instead, we have produced normalized $(1/\omega_0)$ $(\partial\omega/\partial P)_T$ slopes for comparison.

Considering that in a molecular crystal the intramolecular forces are, usually, much stronger than the intermolecular ones, it is expected that internal modes should display higher frequencies, but lower normalized $(1/\omega_0)(\partial\omega/\partial P)_T$ slopes (and Grüneisen parameters γ_T) in comparison to the external ones. In pure molecular crystals, in which intramolecular and intermolecular cohesion is mediated by strong covalent and weak van der Waals forces, respectively, it has been found [28] that the γ_T values of internal modes are an order of magnitude (at least) lower than those of the external ones. This scaling behaviour has been clearly demonstrated [28] in log–log plots of γ_T parameters against frequencies in which the two sets of modes are distinctly grouped. Correlation plots of normalized slopes against frequency were produced [24] for the Raman modes of $DyPO_4$ in log–log and linear–log scales, and although the modes were divided in two groups (internal/external), there was no clear separation of the two sets regarding the normalized-slope values. In the present work, in order to include two modes of $TbPO_4$ which display negative values of reduced slopes, we have produced linear–log plots (figure 5) in which two mode groupings (linear fittings) are evident, in line with the internal/external division proposed in previous studies [2, 12] for rare-earth phosphates. It is seen from figure 5 that only the pressure-independent mode at 185 cm^{-1} falls significantly out of either the internal or external mode groups. The absence of a gap in the normalized-slope values between the internal and external modes for either $TbPO_4$ or $DyPO_4$ implies that these compounds do not behave as typical molecular crystals [28]. Hence, one may conclude that the bonding in rare-earth phosphates is quite different than that of pure molecular crystals. This conclusion is reasonable bearing in mind that the intermolecular Coulomb binding, between Tb^{3+} (or Dy^{3+})

and $(PO_4)^{3-}$ ions, is much stronger than the van der Waals one in pure molecular crystals [28]. The fact the external (pure lattice) modes of $TbPO_4$ and $DyPO_4$ are not significantly more compressible than the internal (covalent bonding) modes, indicates that the long-range Coulomb forces are comparable in magnitude to the strong covalent ones between phosphorus and oxygen atoms. Such a strong intermolecular binding in rare-earth phosphates, as a whole, is compatible with the extended (temperature) ranges of stability displayed by these compounds [4]. Similar normalized slope-pressure plots (like those of figure 5) and internal/external mode divisions have been obtained in similar high-pressure Raman experiments in other zircon-type phosphates (YPO_4, $ErPO_4$, $TmPO_4$).

The evolution of the Raman spectrum of $TbPO_4$ (figure 3) and the relevant frequency–pressure plot (figure 4) reveal that the B_{2g} internal bending mode [1, 2, 12] at 331 cm^{-1} softens with increasing pressure to the extent that a level crossing occurs at about 7.0 GPa with the E_g rotational mode at 293 cm^{-1}. At a higher pressure $P_c \approx 9.5$ GPa, abrupt spectral changes are observed which are manifested by the appearance of several new lines (figure 3) and mode discontinuities (figure 4). The changes at this pressure imply a definite first-order phase transition which is irreversible upon pressure release. Only few Raman modes of the low-pressure phase appear to evolve in a continuous way to a counterpart in the high-pressure phase, so that the spectrum looks completely different above P_c (figure 3). The number of observed Raman mode peaks increases from 11 (tetragonal phase) to, at least, 20 above P_c (figure 4), implying a transition to a lower symmetry structure.

The irreversibility of the phase transition is further demonstrated by separate frequency–pressure plots of phonons of the high-pressure phase which are shown in figure 6. In these plots the data points of the pressure increasing cycle (above P_c) are also incorporated, along with six additional data points (for most phonons) obtained during the pressure decreasing experimental session, three above and three below P_c. In the pressure decreasing cycle, 19 phonons have been observed (figure 6) with $(\partial\omega/\partial P)_T$ slopes similar to those of the increasing pressure session (above P_c), thus confirming the irreversible nature of the phase transition throughout the pressure range. Linear fittings have been obtained for each of the 19 phonons including all experimental points (both cycles) of the high-pressure phase. One extra phonon at about 240 cm^{-1} (at a pressure of ~10.7 GPa) observed weakly in four points of the pressure increasing session, has not been detected in the pressure decreasing one, most likely because of an unfavourable orientation of the crystal inside the DAC during pressure release. Two phonons of the high-pressure phase display almost identical frequencies (~430 cm^{-1}) after pressure release (figure 6) and this might have been considered as an indication of merging of the two species in one; however, we think this is very unlikely as the two phonons differ substantially in intensity so that, having different $(\partial\omega/\partial P)_T$ slopes, the strong phonon obscures observation of the weak one. Comparison between the plots of figures 4 and 6 reveals that the phonons of the high-pressure phase of $TbPO_4$ display lower $(\partial\omega/\partial P)_T$ slopes than the phonons of the low-frequency

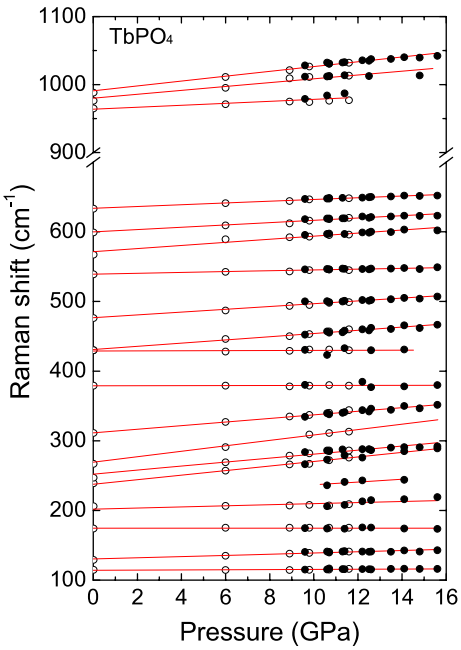

Figure 6. Frequency–pressure plots of the Raman active modes of the high-pressure phase of $TbPO_4$ for the increasing (solid circles) and decreasing (open circles) pressure cycles; linear fittings have been produced for all data points.

tetragonal phase. This slope difference indicates a phase transition to a less compressible (more compact) structure which is compatible with the increase of cation coordination with pressure in ABO_4 compounds [14]. On the other hand, the frequency range spanned by the modes of tetragonal $TbPO_4$ sustains an overall downward shift above 9.5 GPa. This could be interpreted in terms of modifications or distortions of the building units of the crystal.

As mentioned before, most of the zircon-structured compounds studied in the past have shown [14–20] an irreversible first-order phase transition to the scheelite $I4_1/a$ (C^6_{4h}) structure at high pressures. In this structure, 13 Raman active modes are expected (one more than the zircon structure) having the following symmetries: $3A_g + 5B_g + 5E_g$. A zircon-to-scheelite transition does not seem likely in the case of $TbPO_4$ as the number of Raman modes observed in the high-pressure phase (20) is much higher than the 13 modes of the scheelite structure. On the other hand, some zircon-type crystals, though, display [14, 21–23] a first pressure-induced transition to the monoclinic monazite-type $P2_1/n$ (C^5_{2h}) structure in which 36 Raman modes ($18A_g + 18B_g$) are expected. At a first consideration, given that only 20 modes are clearly observed in the high-pressure spectrum of $TbPO_4$, a zircon-to-monazite transition does not look favourable. However, such a transition should not be excluded as the difference in the observed modes may be due to congestion of weak Raman peaks above P_c which prevents their resolution in several occasions. In fact, the spectrum of the high-pressure phase of $TbPO_4$ (figure 3) resembles qualitatively that [2] of the light rare-earth phosphates (La to Gd) which crystallize in the monazite structure [2, 3]. It is recalled that $TbPO_4$ appears also (at ambient conditions) in the monazite-type dimorph [4],

which transforms to the zircon-type at high temperatures, but there are no Raman data available in the literature for the former dimorph. Also, among the heavy rare-earth phosphates, $TbPO_4$ is the closest member to the group of the light ones (La to Gd) and, therefore, it is reasonable to expect that application of pressure will induce a transition to a more compact monoclinic structure. It is worth mentioning that, parallel to $TbPO_4$, we have studied the Raman spectra at high pressures of the isomorphous $ErPO_4$ and $TmPO_4$ compounds, which are distant from the monazite-type, light rare-earth phosphates and do not display dimorphism [4]; there has been no evidence for a phase transition in these compounds up to pressures of 15 GPa, thus confirming the general idea that rare-earth phosphates are stable [4] under high pressure. Although the study of Raman spectra has not provided unambiguous evidence about the structure of the high-pressure phase, there is clear evidence for a first-order irreversible phase transition (to a lower symmetry structure) of $TbPO_4$ at P_c. Based on the above correlations and arguments, we suggest that a strong candidate for the high-pressure modification of $TbPO_4$ is the monoclinic, monazite-type structure.

Finally, we discuss a possible correlation of the anomalous softening of the B_{2g} internal bending mode of tetragonal $TbPO_4$ with the observed phase transition. In their low-temperature Raman studies of zircon-structured $TbVO_4$, $DyVO_4$ and $DyAsO_4$, Elliott *et al* [12] attributed the anomalous softening (with decreasing temperature) of B_{2g} ($TbVO_4$) or B_{1g} ($DyVO_4$, $DyAsO_4$) modes to a distortion of the primitive cell along the [110] or [100] directions, respectively. By analogy, in the process of pressure-induced contraction of $TbPO_4$, it is plausible to expect that a similar structural distortion takes place leading to a deformed zircon structure.

4. Conclusions

Raman measurements have been carried out in tetragonal zircon-type structure $TbPO_4$, both at ambient conditions and at high pressures. Polarized Raman spectra obtained from a single oriented crystal at ambient conditions have allowed us to make symmetry assignments for the 11 observed (out of 12 expected) Raman active modes of tetragonal $TbPO_4$.

From the pressure dependence of Raman spectra of tetragonal $TbPO_4$, plots of normalized $(1/\omega_0)\ (\partial\omega/\partial P)_T$ slopes against mode frequencies have been obtained which show two distinct mode groupings, in agreement with the internal/external division of modes suggested previously [2, 12] for rare-earth phosphates.

Although all reports [4] so far have indicated that rare-earth RPO_4 phosphates are stable under pressures, the high-pressure Raman measurements in tetragonal $TbPO_4$ have provided definite evidence for a first-order structural modification of this crystal at $P_c \approx 9.5$ GPa towards a lower symmetry structure. The high-pressure phase is quenchable upon pressure release and more compact than the zircon one. Unlike most zircon-structured compounds [14–20], it appears that the high-pressure structure of $TbPO_4$ is not the scheelite-type. The Raman spectrum above the phase transition indicates that the monoclinic monazite-type structure is a likely candidate for the high-pressure phase of $TbPO_4$. We suggest that the phase transition at high pressure is related to the B_{2g} symmetry internal bending mode which softens with pressure.

Acknowledgment

We would like to thank the Materials preparation group of Clarendon Laboratory, University of Oxford for providing single crystal samples of $TbPO_4$.

References

[1] Dawson P, Hargreave M M and Wilkinson G R 1971 *J. Phys. C: Solid State Phys.* **4** 240
[2] Begum G M, Beall G W, Boatner L A and Gregor W J 1981 *J. Raman Spectrosc.* **11** 273
[3] Meldrum A, Boatner L A and Ewing R C 1997 *Phys. Rev.* B **56** 13805
[4] Kolitsch U and Holtstam D 2004 *Eur. J. Mineral.* **16** 117 and references therein
[5] Ushakov S V, Helean K B, Navrotsky A and Boatner L A 2001 *J. Mater. Res.* **16** 2623
[6] Suzuki H and Nakajima T 1979 *J. Phys. Soc. Japan* **47** 1441
[7] Nägele W, Hohlwein D and Domann G 1980 *Z. Phys.* B **39** 305
[8] Bluck S and Kahle H G 1988 *J. Phys. C: Solid State Phys.* **21** 5193
[9] Mensinger H, Jakelski J, Kahle H G, Kasten A and Paul W 1993 *J. Phys.: Condens. Matter* **5** 935
[10] Liu G K, Loong C-K, Trouw F, Abraham M M and Boatner L A 1994 *J. Appl. Phys.* **75** 7030
[11] Morin P, Rouchy J and Kazei Z 1994 *Phys. Rev.* B **50** 12625
[12] Elliott R J, Harley R T, Hayes W and Smith S P R 1972 *Proc. R. Soc.* A **328** 217
[13] Gehring G A and Gehring K A 1975 *Rep. Prog. Phys.* **38** 1
[14] Liu L and Bassett W A 1986 *Elements, Oxides, Silicates: High-Pressure Phases with Implications for the Earth's Interior, Oxford Monographs on Geology and Geophysics* No 4 (Oxford: Clarendon) and references therein
[15] Kusaba K, Yagi T, Kikuchi M and Syono Y 1986 *J. Phys. Chem. Solids* **47** 675
[16] Jayaraman A, Kourouklis G A, Espinosa G P, Cooper A S and Van Uitert L G 1987 *J. Phys. Chem. Solids* **48** 755
[17] Wang X, Loa I, Syassen K, Hanfland M and Ferrand B 2004 *Phys. Rev.* B **70** 064109
[18] Duclos S J, Jayaraman A, Espinosa G P, Cooper A S and Maines R G Sr 1989 *J. Phys. Chem. Solids* **50** 769
[19] Long Y W, Zhang W W, Yang L X, Yu Y, Yu R C, Ding S, Liu Y L and Jin C Q 2005 *Appl. Phys. Lett.* **87** 181901
[20] Long Y W, Yang L X, Yu Y, Li F Y, Yu R C, Ding S, Liu Y L and Jin C Q 2006 *Phys. Rev.* B **74** 054110
[21] Fukunaga O and Yamaoka S 1979 *Phys. Chem. Minerals* **5** 167
[22] Range K-J, Meister H and Klement U 1990 *Z. Naturf.* b **45** 598
[23] Liu L 1982 *Earth Planet. Sci. Lett.* **57** 110
[24] Kontos A G, Stavrou E, Malamos V, Raptis Y S and Raptis C 2007 *Phys. Status Solidi* b **244** 386
[25] Becker P C, Edelstein N, Williams G M, Bucher J J, Russo R E, Koningstein J A, Boatner L A and Abraham M M 1985 *Phys. Rev.* B **31** 8102
[26] Hirch K R and Holzapfel W B 1981 *Rev. Sci. Instrum.* **52** 149
[27] Watson G H Jr, Daniels W B and Wang C S 1981 *J. Appl. Phys.* **52** 956
[28] Weinstein B A and Zallen R 1984 *Light Scattering in Solids IV* (*Springer Topics in Applied Physics* vol 54) ed M Cardona and G Güntherodt (Berlin: Springer) p 463